Available online at www.sciencedirect.com

ScienceDirect

journal homepage: http://www.elsevier.com/locate/acme

Original Research Article

Energetic efficiency of gear micropumps

W. Kollek, U. Radziwanowska *

Institute of Machines Design and Operation, Wroclaw University of Technology, Poland

ARTICLE INFO

Article history:
Received 3 December 2013
Accepted 16 May 2014
Available online 20 June 2014

Keywords:
Gear micropump
Energetic efficiency
Pump body FEM analysis

ABSTRACT

In this paper, results of the static mechanical analysis of a gear micropump body are presented. Numerical simulations using finite element method (FEM) were conducted using Ansys Multiphysics software. After analysis of stress and displacement distribution in the pump body, a mass optimization of construction was provided. In the optimized body, maximal value of stress reached 134 MPa. Safety factor was equal to 2.9. The highest value of displacement in the optimized body was about 0.02 mm. Maximal values of stress and displacement provide appropriate work of the micropump. Strength and stiffness criteria in the optimized pump body were achieved. For the construction of the pump body before and after optimization, energetic efficiency ratios (k_{ef}) were calculated. Optimized micropump body has more than 30% increase in k_{ef} ratio to the pump with the primary body.

1. Introduction

Nowadays, pumps are the most common machines and are used in all fields of technology. Among the displacement pumps used in hydraulic drive systems as power generators, gear pumps are the most common. Their usage share is estimated at more than a half of all manufactured pumps. The major advantages of gear pumps and motors include: a simple and compact design, reliability, resistance to working medium impurities, high efficiency, and small size in comparison with other pumps. The design of the gear pump has evolved over the last 400 years (the creator of the first gear unit was Johannes Kepler, who patented his solution in 1604). In the literature, large variety of different constructions with the hydraulic and acoustic properties improvement can be found [9,16,18,20]. Currently, the development of modern gear units is associated with the following directions: increase in working pressures [7,18,22], overall efficiency improvement [1,3,4,8,16], reduction of pressure pulsations [2,18,22], weight [12,16] and noise minimization [15,17,19] and reduction of dynamic loads [9,13,14,20,21].

In recent years, a dynamic progress in the field of microelectronics and micromechanics has created new opportunities for the development of fluid power microsystems and microhydraulics. Miniaturization of hydraulic elements allows replacing the classical hydraulics with microhydraulics, where due to size or weight the former cannot be applied. There are three main factors to determine the classification of pump as a micropump. They are overall dimensions, nominal size and rate of flow. The dimensions of microhydraulic pumps imparting the required flow and pressure to the liquid range from a few hundred nanometers to a few centimeters. The nominal size, which for displacement pumps refers to specific delivery, for microhydraulic components needs to be below 6 (NM < 6). The flow rate in

* *Corresponding author*. Tel.: +48 71 320 27 00.
E-mail address: urszula.radziwanowska@pwr.wroc.pl (U. Radziwanowska).
http://dx.doi.org/10.1016/j.acme.2014.05.005

microhydraulics may be small, 2–50 cm^3/s (120–300 cm^3/min), or very small, <2 cm^3/s (<120 cm^3/min) [5,6,11].

The minimization of pump weight largely affects the geometry of the body. On the other hand, too large "trim" of the structure can lead to a reduction in its strength below the limit value resulting from the normal operation of the gear unit. It follows that the design of the pump requires solving a problem of optimal geometry of the pump body so that it was characterized by the smallest possible dimensions and weight while maintaining all the criteria of strength. The pump design analyzed in this paper belongs to a group of microhydraulic elements, since the overall dimensions are height – 56 mm, width – 52 mm, and length (for the biggest pump from type series) – 56.3 mm. It is characterized by a small flow, up to 25 cm^3/s, and specific delivery equals 1 cm^3/rev; therefore NM < 6. Moreover, the values of specific delivery of most recently produced gear pumps meet the requirements of numbers based on preferred numbers (preferred values), developed in the XIX century by Charles Renard. Currently, according to the generally accepted standard, micropumps belong to group 0, in which specific delivery is up to 1 cm^3/rev. Therefore, for numerical calculations in this article, the micropump of the highest specific pump delivery of 1 cm^3/rev was chosen, since the pump body in this case is the most strained.

2. FEM analysis of gear micropump body

2.1. Geometric model

During the implementation of developmental grant no. 03 0032 04/2008 the type series of gear micropumps PZ0 were designed and manufactured [10]. The prototype units have a three-part structure, which are a flange, pump body and back cover. A flange is used to attach the micropump to drive assembly. In the pump body are placed drive and idler gears – the pumping unit, bushings, and the suction and pressure ports for connection to the drive system. The entire structure closes the back cover. In the flange and back cover, compensation and anti-extrusion seals are placed to prevent the leakage. The panels are interconnected with four bolts. Their mutual axial position is secured by dowel pins. The exploded view of the micropump design is shown in Fig. 1.

On the basis of a previously prepared technical documentation of gear micropump (Fig. 2), a 3D model of the pump body was prepared. The model was created in Autodesk Inventor software (Fig. 3), saved as *parasolid* file, and then imported into Ansys Multiphysics environment. In the model geometry, minor simplifications were done, e.g. in the suction and pressure channel the thread was not included. A highly detailed model may cause serious difficulties in the preparation of a discrete model, as it forces higher density of the discrete elements grid. This in turn increases the number of elements, the computation time and requires a higher usage of computer memory. It was found that the geometry simplification will not significantly affect the results of the simulation. For the analysis, the largest dimensions from the pump type series were used. The central body due to the longest length is the most strained, as discharge pressure impacts the largest area.

2.2. Discrete model

The geometric model was divided into tetrahedral finite elements of higher order (solid187). Each element is defined by 10 nodes – at the vertices and at each edge of the tetrahedron. The element is suited to modeling irregular meshes, especially for various geometry from CAD/CAM systems. Each node of this element has three degrees of freedom allowing translational movement in x, y and z directions. The grid elements ensure high accuracy of the calculations in the case of a complex geometry model [23]. Finite element mesh is refined inside the pump body on the contact area of the body with bushings and in the discharge port (Fig. 4).

2.3. Material properties

The pump housing is made of aluminum alloy PA6. This alloy is characterized by good strength properties and a high tensile and fatigue strength. Mechanical and physical properties of the alloy according to PN-84/H-93669 PA6 are summarized in Table 1.

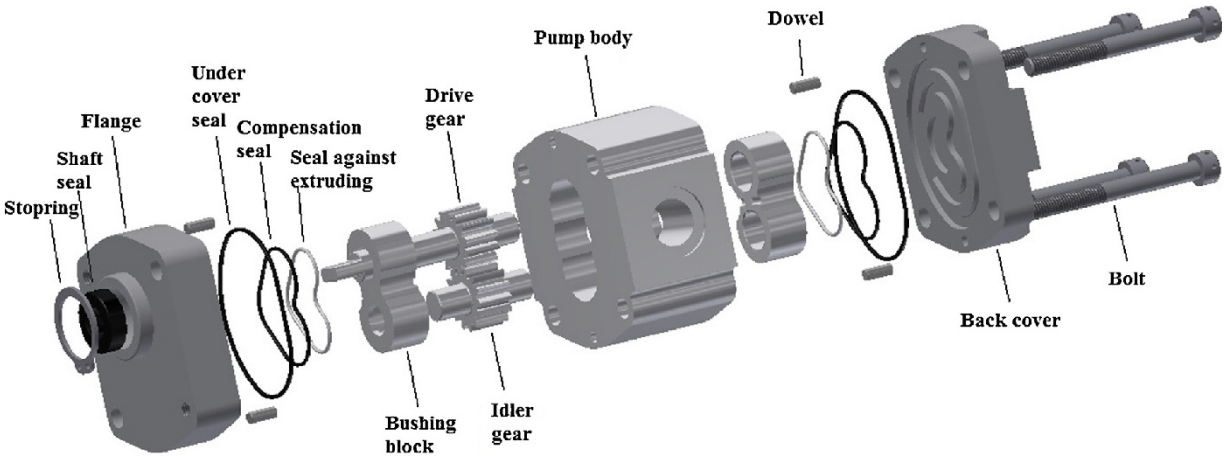

Fig. 1 – Elements of the gear micropump.

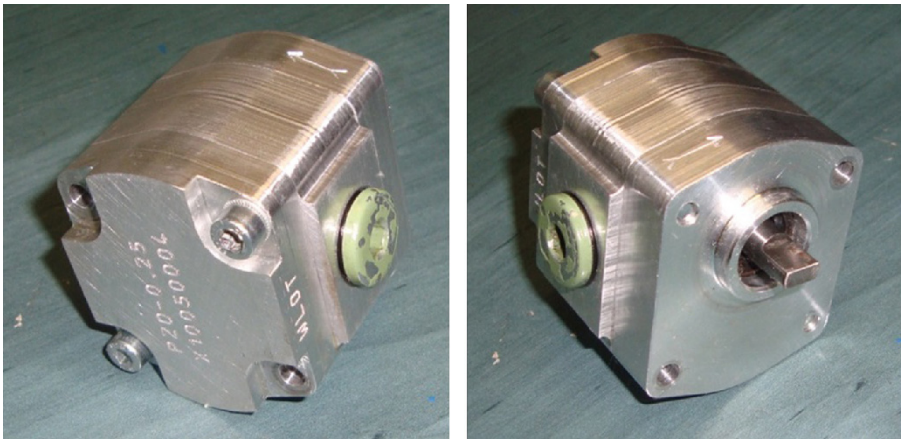

Fig. 2 – Photography of pump PZ0 prototype.

2.4. *Loads and boundary conditions*

In the pump model, following loads are assumed:

- a zone of linear pressure increase and discharge pressure zone in the channels of displacement,

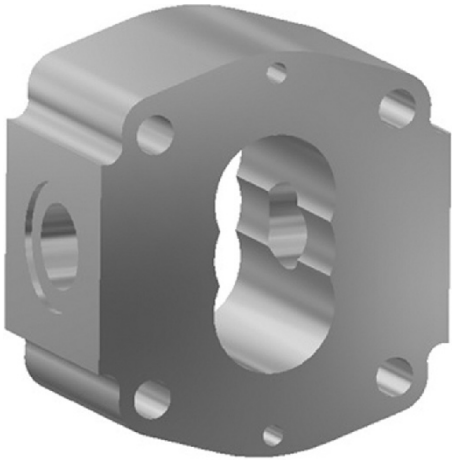

Fig. 3 – Geometric model of gear micropump body.

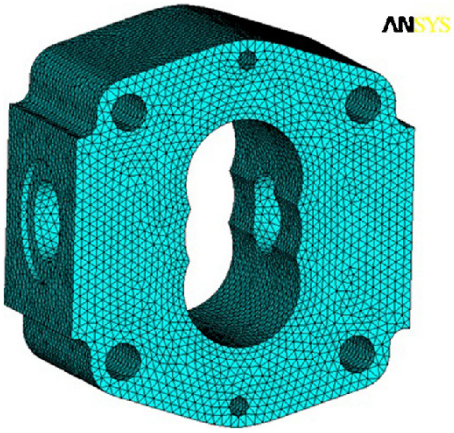

Fig. 4 – Discrete model of gear micropump body.

- a zone of discharge pressure at the discharge port,
- a zone of bearing pressure on the pump body.

In the analyzed construction of the pump body, the angles $\alpha_1 = 81^\circ$ and $\alpha_2 = 154^\circ$ are assumed (Fig. 5). The values for the particular angles were determined based on the conducted measurements of peripheral pressure [18]. In the range of α_2–α_1 pressure increases linearly from 0 MPa to 28 MPa. In the remaining part, the value of pressure is constant and equal to 28 MPa. The suction pressure is negligibly small compared with the discharge pressure, and therefore was not included. The body was loaded symmetrically on the side of drive and idler gear. Reaction force on the gear bearing was determined from Eq. (1):

$$R = \frac{0.85\,pbd_w}{2} = 1860N \tag{1}$$

where p – pressure, $p = 28$ MPa, b – face width of gear, $b = 9.3$ mm, and d_w – tip (addendum) circle diameter, $d_w = 16.8$ mm.

The model is fixed in the four holes for screws connecting the body elements according to literature [12]. All the translations in x, y, and z directions in the nodes of this elements are set to zero. The reason for fixing screw surfaces in all directions is that the pump assembly does not allow the pump body to move in any direction. In the vertical (Y) and horizontal (X) axes, the move of the pump is constrained by bolts and dowels. In the third axis (Z, toward the viewer) it was assumed that the pump body could not move, as it results from being tightly bolted together to the flange, and back cover. However, in this direction a slight movement might be

Table 1 – Properties of aluminum alloy PA6.

Property (unit)	Value
Tensile strength, R_m (MPa)	390
Yield strength, $R_{0.2}$ (MPa)	250
Density, ρ (g/cm^3)	2.79
Tensile modulus, E (MPa)	72,500
Poisson's ratio, ν (–)	0.33

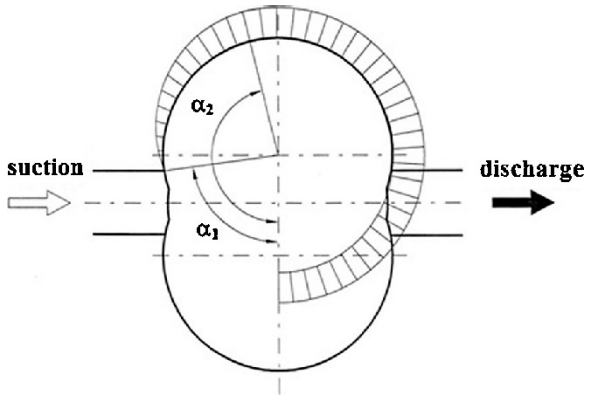

Fig. 5 – The schematic of pressure distribution in the interior chamber for pumping.

included. It has been tested that enabling the movement in Z axis for 0.1 mm or even 0.5 mm does not significantly influence the results (the maximal stress value in the pump body was decreased by almost 2 MPa while including a movement of 0.5 mm).

3. Results of FEM analysis

Strength calculations in the field of linear static analysis with the aid of the finite element method were carried out. In the model of the pump housing, distribution of reduced stress according to Huber–Mises hypothesis and distribution of displacement vector sum were observed. The results of stress and displacement distribution are shown in the form of contour plots in Figs. 6 and 7.

When analyzing the distribution of stress as shown in the contour plot (Fig. 6), the greatest amount of stress 92 MPa may be seen. The concentration of stress values occurs in the place of bushing blocks in the interior part of the pump body on the discharge side. High values of the stress occur in the periphery of the discharge channel inside the pump body and in the vicinity of screw holes on the right side of the body. The value

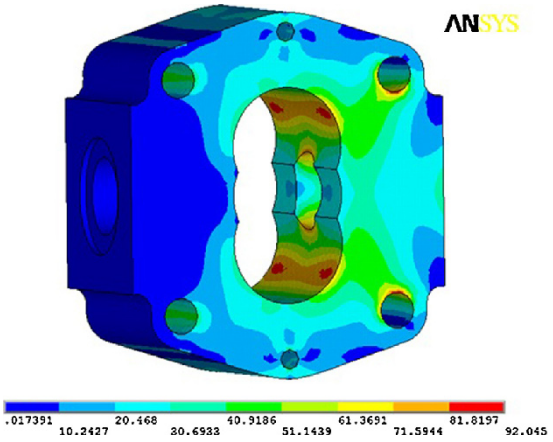

Fig. 6 – Stress distribution in gear micropump body before optimization.

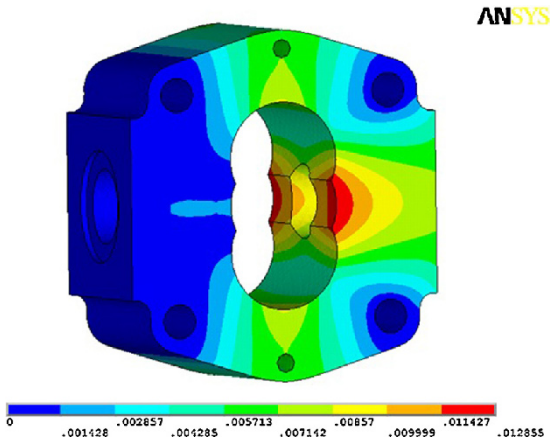

Fig. 7 – Displacement distribution in gear micropump body before optimization.

of the maximum stress is considerably less than the yield strength of aluminum alloy (250 MPa) and the tensile stress (390 MPa). Safety factor in this case is 4.2.

$$n = \frac{\sigma_n}{\sigma} = \frac{390}{92} \approx 4.2 \tag{2}$$

In the remaining part of the body, stress values are much smaller than the maximum value and are in the range of 10–50 MPa. On the side of the suction channel, stress values are close to zero.

As shown in Fig. 7, the largest displacement value is approximately 0.013 mm. The maximal displacement occurs on the discharge channel side on the inside of the pump housing. In other areas, the displacement of the pump body is smaller than 0.01 mm. The maximum value of the displacement occurring in the body does not exceed the clearance limit values specified in the papers [9,18]. Strength and stiffness criteria in the pump body are achieved.

4. Optimization of gear micropump body

The results of simulations carried out on the model of the gear pump housing have shown that the stress and displacement values in the model are much smaller than the limit value. Therefore, it was decided to optimize the weight of the body structure of the pump. The goal of optimization was to achieve higher energetic efficiency ratio (P/m) of the pump while maintaining the same overall efficiency. Therefore, the pumping unit, bushings, and the suction and discharge port size were not changed. Also the material of construction has not been subjected to change. The criterion of optimization was the smallest mass of the micropump body. The variables of optimization were the overall dimensions of micropump body, stress and displacement distributions in the housing. The dimensions of the micropump housing should be as small as possible while the stress and displacement values vary in an acceptable range. For stress, maximal value of 159 MPa was assumed, as the safety factor then equals 2.5. High value of safety factor needs to be assumed, as in the model some

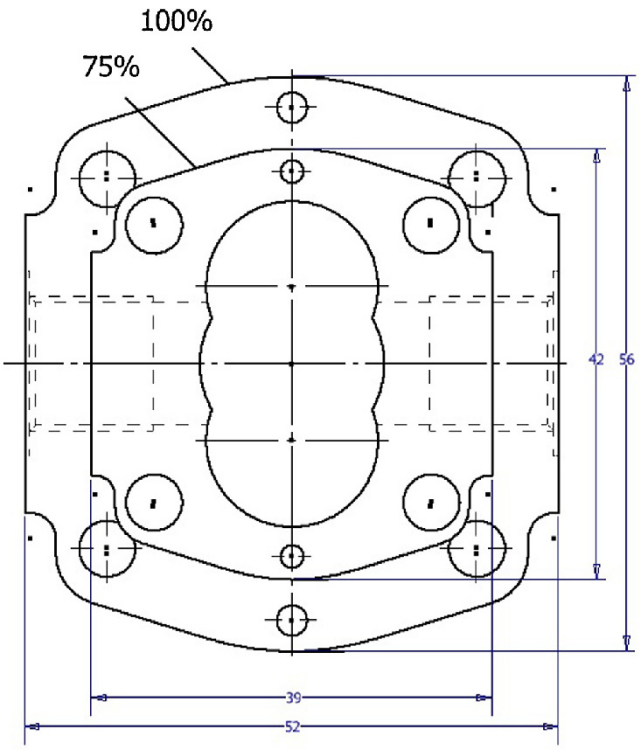

Fig. 8 – Comparison of the pump body size before optimization (100%) and after optimization (75%).

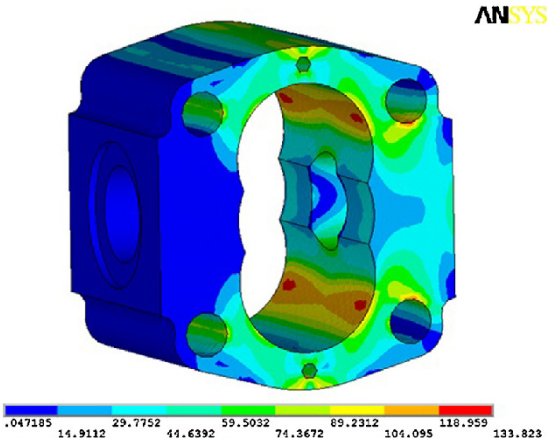

Fig. 9 – Stress distribution in gear micropump body after optimization.

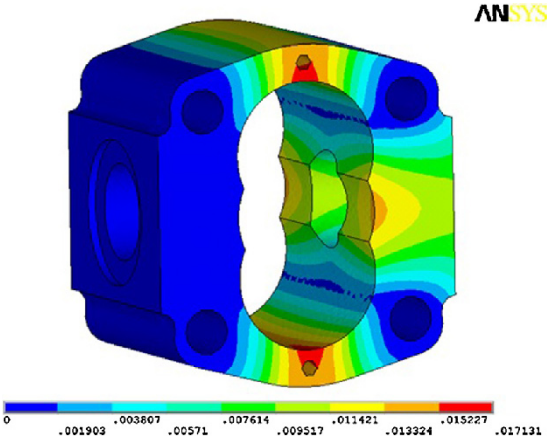

Fig. 10 – Displacement distribution in gear micropump body after optimization.

simplifications were applied and FEM analysis is always vitiated by an error. The maximal displacement value should not exceed 0.02 mm, as displacement in the range from 0.1 to 0.2 mm refers to circumferential backlash and does not have a negative impact on volumetric efficiency. Overall output dimensions of the body were reduced by 25% while maintaining the shape and fixed dimensions – the size of the suction and discharge channel and the size of the bearing body (Fig. 8). Discrete model, load and constraints were set analogically as in the base model. After the simulation was done, it was noticed that in the dowel holes, maximal values of stress occurred (214 MPa). At these locations, plastic deformation could occur, and therefore the size of the holes was reduced from 3 mm to 2 mm. The results of the numerical simulations for the optimized model are presented in the form of contour plots in Figs. 9 and 10.

In Fig. 9, the distribution of stress in the optimized structure of the body is shown. The highest stress value is about 134 MPa and it occurs in the contact area of the pump body and the bushing blocks and along the edges of holes for fastening screws on the discharge side of the body. Safety factor for this case is 2.9.

$$n = \frac{\sigma_n}{\sigma} = \frac{390}{134} \approx 2.9 \tag{3}$$

An analysis of the displacement map (Fig. 10) shows that the maximum values of displacement occur near the dowel pinholes, and the values reach 0.017 mm. In the rest of the pump body, displacement values do not exceed 0.015 mm. The maximal value of displacement is included in the range acceptable to provide proper conditions for the pump work [9,18]. The optimized design of the pump housing fulfills strength and stiffness criteria.

Assumed safety factor and the obtained maximum values of stress and displacement are similar to the results included in the literature [12].

5. The energetic efficiency ratio of gear micropump

As the result of the gear micropump body optimization, the dimensions and mass of the structure were significantly reduced. The body mass before optimization was about 150 g, while after the reduction of the overall dimensions, it was only about 63 g. Body mass of the original pump body (pump body I), the optimized body (pump body II) and mass of the entire pump with pump body I and pump body II are compared in Table 2.

For both pump bodies, energy efficiency ratio (k_{ef}) was designated. The energetic efficiency ratio is defined as the relation of the power to the mass of the pump (4):

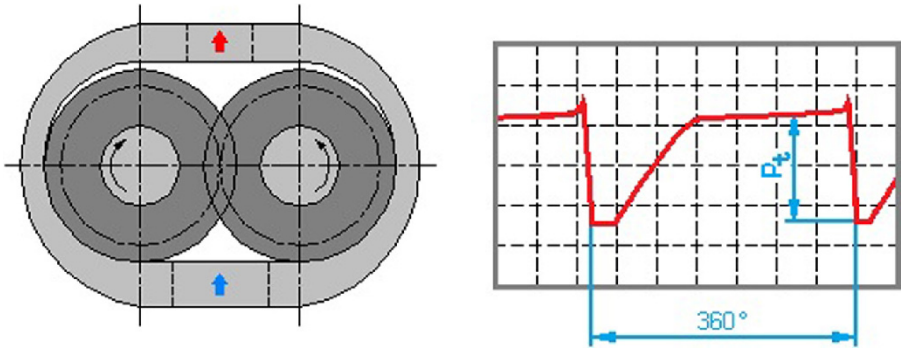

Fig. 11 – Schematic of circumferential sealing of gears and graph of circumferential pressure measured in tooth space [9].

$$k_{ef} = \frac{P}{m} \tag{4}$$

Theoretical delivery of the pump was calculated from the Eq. (5):

$$Q = qn = 1.5\ \mathrm{dm^3/min} \tag{5}$$

where q – specific (unit) delivery, $q = 1\ \mathrm{cm^3/rev} = 1 \times 10^{-3}\ \mathrm{dm^3/rev}$, and n – angular velocity, $n = 1500$ rpm.

Pump power was calculated from Eq. (6):

$$P = Q\,p = 700\,\mathrm{W} \tag{6}$$

where Q – theoretical delivery of the pump, $Q = 1.5\ \mathrm{dm^3/min} = 25 \times 10^{-6}\ \mathrm{m^3/s}$, and p – pressure, $p = 28\ \mathrm{MPa} = 28 \times 10^6$ Pa.

The calculation of the energetic efficiency of the original pump body (7):

$$k_{ef\,I} = \frac{P}{m_I} = \frac{700}{383} \approx 1.8 \tag{7}$$

The calculation of the energetic efficiency of the optimized pump body (8):

$$k_{ef\,II} = \frac{P}{m_{II}} = \frac{700}{297} \approx 2.4 \tag{8}$$

In Table 3, the energetic efficiency ratios of the pump body before and after the optimization are summarized.

On the basis of the calculation, it may be seen that the optimized pump body has 33% higher power to mass ratio than the original pump body. In the modernized pump body, the overall dimensions were reduced by 25%; but the size of the pumping unit (drive and idler gears), bushings, and diameters of suction and discharge ports are maintained unchanged. The efficiency of a gear pump is determined mostly by its radial and face clearance. The radial clearance refers to circumferential backlash and ranges from 0.01 to 0.03 mm. The circumferential clearance is formed by the surface of the gouge in the casing and the surface of a cylinder having the radius of the displacer addendum circle. The circumferential clearance is not constant along the whole circumference, as the gears often get displaced within the bearings, because of their slackness, toward suction port. The gears rotate in the direction opposite to the pressure drop, which results in reducing the leakage due to the difference in pressure at the ends of clearance (Fig. 11).

The increase of radial clearance to 0.017 mm, which is the maximal displacement value and occurs near dowel holes, will not affect the volumetric efficiency of the micropump. The face clearance is by an order of magnitude larger than the radial clearance, amounting from 0.1 to 0.3 mm. To ensure high efficiency of gear pump, axial clearance compensation is performed, both in the primary pump and in the pump with modified body. To sum up, the change of micropump body dimensions should not negatively affect the total efficiency of the micropump.

The compensation surfaces should remain in the same size, as driving unit dimensions were not diminished. Nevertheless, overall dimensions, of flange and back cover of the micropump, should be reduced, to fit the pump body shape. The power to mass ratio was calculated for the micropumps of the same volumetric efficiency, and therefore, in this case the parameter is reliable. While comparing the energetic efficiency ratios of the pumps, the high total and volumetric efficiency should be taken under consideration. In other way, the pump design from the beginning does not meet the basic criterion for positive displacement pumps, which is the high overall efficiency (above 0.9).

Table 2 – Micropump mass comparison before and after optimization.

Parameter	Pump body I (before optimization)	Pump body II (after optimization)
Mass of pump body (g)	149	63
Mass of entire pump (g)	383	297

Table 3 – The comparison of energetic efficiency ratios of the pump body before and after the optimization.

Energetic efficiency	Pump body I (before optimization)	Pump body II (after optimization)
k_{ef} (kW/kg)	1.8	2.4

6. Conclusions

The calculations of gear micropump body structure strength were conducted. On the basis of FEM stress analysis, it was found that both the original body design and an optimized

body gear micropump satisfy the strength and stiffness criteria under working discharge pressure equal to 28 MPa. The highest values of stress in the body of the original gear pump reached 92 MPa. The displacement in the pump body achieved a maximum value of 0.013 mm. The maximum values of stress and displacement obtained in the numerical simulations were much smaller than the limit value; therefore, the optimization of pump body structure was made. As a result of the FEA analysis of optimized pump body, a maximum value of stress of 134 MPa was obtained, while the maximum value of the displacement was 0.017 mm. The maximum displacement value should not have a negative impact on the leak tightness of the pump during its work. Significant values of displacement in the pump body occurred on the areas in which the pressure at the circumference of the gears was no longer incremented [9,18]. Thus, a slight increase in the gap between the tip of the tooth and the body of the pump will not affect its volumetric efficiency. After optimization of the body, the weight of the structure was significantly reduced. The weight of the optimized pump body was more than 50% less than the weight of the original pump body. Reducing the weight of the pump housing while maintaining the mechanical properties is important for the production process due to the possibility of increasing the efficiency of production and reducing the demand for material and thus reducing the production price of the pump. The energetic efficiency ratios of micropumps were determined. The micropump with original body is characterized by a energetic efficiency ratio equal to 1.8, while for the micropump with a modernized body this ratio equals 2.4. It follows that the pump with the optimized body is characterized by more than 30% increase in energy efficiency ratio in comparison to the pump body before optimization. In this case, it means that the pump with lower weight may achieve the same driving power as the pump about 90 g heavier. The analysis does not take into account the pressure pulsation and an increase of oil temperature during work, which also has an impact on the effort of the pump housing during operation. Therefore, high values of the safety factor ($n \approx 3$) were assumed. As part of further research a verification of the obtained results is provided by experimentally measuring the stress values in the pump bodies of prototype units.

REFERENCES

[1] P. Casoli, A. Vacca, G.L. Berta, Optimization of relevant design parameters of external gear pumps, in: 7th International Symposium on Fluid Power, Toyama, 2008.

[2] P. Casoli, A. Vacca, G. Franzoni, A numerical model for the simulation of external gear pumps, in: 6th JFPS International Symposium on Fluid Power, Tsukuba, 2005.

[3] R. Castilla, P.J. Gamez-Montero, N. Erturk, A. Vernet, M. Coussirat, E. Codina, Numerical simulation of turbulent flow in the suction chamber of a gearpump using deforming mesh and mesh replacement, International Journal of Mechanical Sciences 52 (2010) 1334–1342.

[4] S. Dhar, A. Vacca, A novel CFD – axial motion coupled model for the axial balance of lateral bushings in external gear machines, Simulation Modelling Practise and Theory 26 (2012) 60–76.

[5] R. Dindorf, J. Wołkow, Microhydraulics, Hydraulics and Pneumatics (6/99) (1999) 16–19 (in Polish).

[6] R. Dindorf, J. Wołkow, Microhydraulics in Automotive Vehicles, vol. 20, Portfolio of Motorization Scientific Problems Committee, 2000, (in Polish).

[7] I. Ghionea, A. Ghionea, G. Constantin, CAD – CAE methodology applied to analysis of a gear pump, Proceedings in Manufacturing Systems 8 (1) (2013).

[8] G. Houzeaux, R. Codina, A finite element method for the solution of rotary pumps, Computers & Fluids 36 (2007) 667–679.

[9] W. Kollek, P. Osiński, Modelling and Design of Gear Pumps, Wroclaw University of Technology Publishing House, Wroclaw, 2009.

[10] W. Kollek, P. Osiński, M. Stosiak, A. Wilczyński, P. Cichoń, Problems relating to high-pressure gear micropumps, Archives of Civil and Mechanical Engineering 14 (1) (2013) 88–95.

[11] W. Kollek, Fundamentals of design, modeling, operating of microhydraulic elements and systems, Wroclaw University of Technology Publishing House, Wroclaw, 2011 (in Polish).

[12] H. Li, Ch. Yang, P. Zhou, The finite element analysis and optimizations of shells of internal gear pump based on Ansys, Fluid Power and Mechatronics (2011) 185–190.

[13] E. Mucchi, G. Dalpiaz, Experimental validation of a model for the dynamic analysis of gear pumps, in: 25th International Conference on Design Theory and Methodology, ASME, Portland, Oregon, USA, 2013.

[14] E. Mucchi, G. Dalpiaz, A. Fernandez del Rincon, Elastodynamic analysis of a gear pump. Part I: Pressure distribution and gear eccentricity, Mechanical Systems and Signal Processing 24 (2010) 2160–2179.

[15] E. Mucchi, A. Rivola, G. Dalpiaz, Modelling dynamic behaviour and noise generation in gear pumps: procedure and validation, Applied Acoustics 77 (2014) 99–111.

[16] P. Osiński, A. Deptuła, M.A. Partyka, Discrete optimalization of a gear pump after tooth root undercutting by means of multi-valued logic trees, Archives of Civil and Mechanical Engineering 13 (4) (2013) 422–431.

[17] P. Osiński, W. Kollek, Assessment of energetistic measuring techniques and their application to diagnosis of acoustic condition of hydraulic machinery and equipment, Archives of Civil and Mechanical Engineering 13 (3) (2013) 313–321.

[18] P. Osiński, High-Pressure and Low-Pulsation External Meshing Gear Pumps, Wroclaw University of Technology Publishing House, Wroclaw, 2013 (in Polish).

[19] P. Osiński, Modelling and Design of Gear Pumps with Modified Tooth Profile, LAP Lambert Academic Publishing, Saarbrucken, 2014.

[20] C. Ragunathan, C. Manoharan, Dynamic analysis of hydrodynamic gear pump performance using design of experiment stand operational parameters, IOSR Journal of Mechanical and Civil Engineering 1 (6) (2012) 17–23.

[21] A. Vacca, M. Guidetti, Modelling and experimental validation of external spur gear machines for fluid power applications, Simulation Modelling Practice and Theory 19 (2011) 2007–2031.

[22] S. Wang, H. Sakurai, A. Kasarekar, The optimal design in external gear pumps and motors, ASME Transactions on Mechatronics 16 (5.) (2011).

[23] http://www.kxcad.net/ansys/ANSYS/ansyshelp/Hlp_E_SOLID187.html.